Control of Petersen Coils

Gernot Druml, *Member, IEEE*, **Andreas Kugi**, *Member, IEEE*, **Bodo Parr**

***Abstract*--In this paper we present a new method for the control of Petersen coils in resonant grounded networks. The major problem for the tuning at small neutral-to-earth voltages is to distinguish between resonance points simulated by the disturbances and real resonance points. In addition the controller has to recognize network modifications during the tuning operation. The first part of this contribution is a short description of the essential parameters that define the resonance curve. The second part deals with the disturbances at very small neutral-to-earth voltages. In consideration of these disturbances a new algorithm is presented to improve the accuracy of the tuning operation of the Petersen coil.**

Index Terms -- Petersen coil, resonant grounding, transmission lines.

I. Introduction

THE "resonant grounding" is one of the most important options in electrical network design to obtain the optimal power supply quality. The main advantage of the treatment of the neutral point is the possibility of continuing the network operation during a sustained earth-fault. As a consequence this reduces the number of interruptions of the power supply for the customer.

For the suppression of the arc the Petersen coil should be well tuned within limits, which are described in [1] and [9] for the different insulation levels. The increase in the cable lengths of distribution networks brings about that on the one hand the level of the neutral-to-earth voltage is decreasing and on the other hand the resonance curves become sharper. The reason for the reduction of the neutral-to-earth voltage level is mainly due to the reduced capacitance tolerances of the new cables. Furthermore, the cables have smaller losses compared to equivalent overhead lines. This is why, the damping of the network is reduced and the resonance curves become sharper.

A first idea to meet these new demands on the control of Petersen coils is to make the measurement of the neutral-to-earth voltage more sensitive. But in this paper we will show that with this idea we do not get satisfactory results. The main reason for this is that the disturbances caused by the system due to, e.g. geometrically asymmetric installed cables, are higher than the measurement noise. Therefore, we will direct our attention to elaborate the reasons for the different disturbances of the neutral-to-earth voltage. Finally, a new approach for finding the resonance point also for smaller neutral-to-earth voltage levels will be presented.

Gernot Druml is working with a-eberle gmbh in Nuremberg, Germany (e-mail: g.druml@ ieee.org).
Andreas Kugi is with the Department of Automatic Control and Control Systems Technology of the Johannes Kepler University in Linz, Austria (e-mail: kugi@mechatronik.uni-linz.ac.at).
Bodo Parr is working in the research group of a-eberle gmbh in Nuremberg, Germany (e-mail: bodo.parr@a-eberle.de).

II. Basics of the Resonant Grounding

A. Principals of the resonant grounding

In medium-voltage (MV) and high-voltage (HV) networks with "resonant grounding" the current over the fault location in the case of a single line-to-earth-fault (SLE) is reduced by the use of the Petersen coil. For this the Petersen coil is adjusted during the sound operation of the network to compensate the capacitive current over the fault location by an inductive current. Fig. 1 shows the simplified equivalent circuit used for a faulty distribution system where we assume ideal symmetrical three-phase voltage sources and negligible line resistances and inductances.

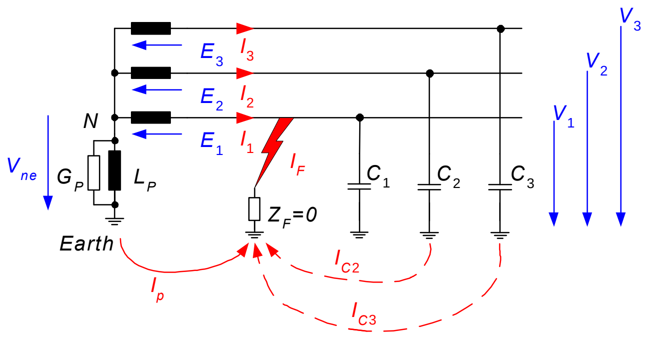

Fig. 1. Simplified equivalent circuit for the "resonant grounding".

The phasor diagram of fig. 1 for a SLE with $Z_F = 0\ \Omega$ is depicted in fig. 2a. The situation of different coil positions of the Petersen coil and the resulting current I_F over the fault location are shown in fig. 2b.

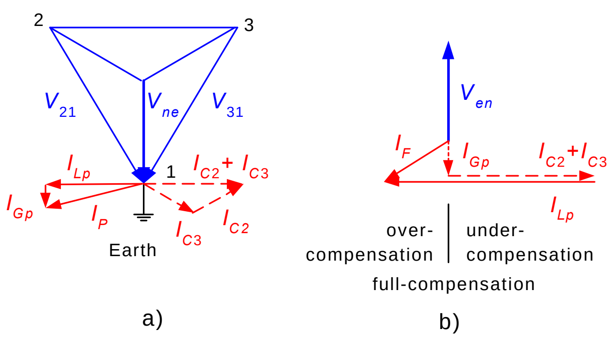

Fig. 2. a) Phasor diagram for a single line-to-earth-fault (SLE).
b) Reduced phasor diagram.

L_P, G_P	Petersen coil (inductance, conductance)
C_1, C_2, C_3	line-to-earth capacitances
Z_F	impedance at the fault location
N	star point of the transformer (neutral point)
E_1, E_2, E_3	phase voltages
V_{ne}	neutral-to-earth voltage
I_{C2}, I_{C3}	capacitive current of the two sound lines
I_P	current of the Petersen coil
I_{GP}	wattmetric part of I_P
I_{LP}	inductive part of I_P
I_F	current over the fault location

For the derivation of the mathematical model the following assumptions will be made (see fig. 3):

- The line-to-earth capacitances and conductances are symmetrical and
- the line-unbalance (capacitive and ohmic) is reduced to phase 1.

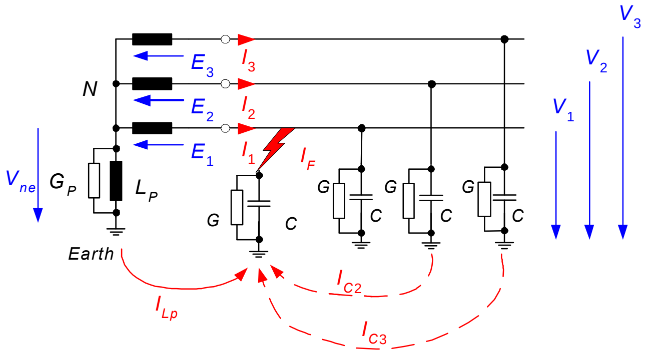

Fig. 3. Simplified equivalent circuit.

For the equivalent circuit of fig. 3 the following equations

$$0 = I_P + I_1 + I_2 + I_3 \quad (1)$$

$$V_{ne} Y_P = I_P \quad (2)$$

$$(E_1 + V_{ne}) Y_1 = I_1 \quad (3)$$

$$(E_2 + V_{ne}) Y_2 = I_2 \quad (4)$$

$$(E_3 + V_{ne}) Y_3 = I_3 \quad (5)$$

Hold, with the admittances

$$Y_P = G_P + \frac{1}{jwL_P} \quad (6)$$

$$Y_1 = (G + \Delta G) + jw(C + \Delta C) \quad (7)$$

$$Y_2 = Y_3 = G + jwC. \quad (8)$$

Assuming a symmetrical three-phase system and using the abbreviation $a = e^{-j120°}$ with $0 = 1 + a + a^2$, we can write the voltages E_2 and E_3 in the form

$$E_2 = a^2 E_1 \quad \text{and} \quad E_3 = aE_1 \ . \quad (9)$$

Now eq. (1) yields to

$$0 = V_{ne}(Y_P + Y_1 + Y_2 + Y_3) + E_1(Y_1 + a^2 Y_2 + aY_3) \quad (10)$$

or equivalently

$$V_{ne} = -\frac{Y_1 + a^2 Y_2 + aY_3}{Y_P + Y_1 + Y_2 + Y_3} E_1 . \quad (11)$$

Using eqs. (6) - (8), we get

$$Y_1 + a^2 Y_2 + aY_3 = \Delta G + jw\Delta C \quad (12)$$

$$Y_1 + Y_2 + Y_3 = (3G + \Delta G) + jw(3C + \Delta C) \quad (13)$$

and hence eq. (11) results in

$$V_{ne} = -\frac{Y_U}{Y_U + Y_W + j(B_C - B_L)} E_1 = -\frac{Y_U}{Y_U + Y_O} E_1 \quad (14)$$

with

$Y_U = \Delta G + jw\Delta C$	unbalance of the fault location
$Y_W = 3G + G_P$	wattmetric part of Y_O
$B_C = w3C$	capacitive part of Y_O
$B_L = \frac{1}{wL_P}$	inductive part of Y_O .

The equivalent circuit of eq. (14) is depicted in fig. 4. This circuit is valid for low ohmic single line-to-earth-faults as well as for the natural capacitive unbalance of the sound network provided that the previous assumptions are satisfied.

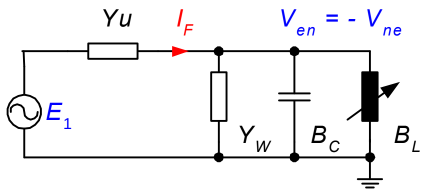

Fig. 4. Single phase equivalent circuit for the “resonant grounding”.

In the following subsections the dependence of V_{ne} and I_F on the tuning of the Petersen coil under the two major operation conditions will be discussed.

B. Low ohmic single line-to-earth-fault:

In the case of a low ohmic earth-fault the capacitive unbalance jB_C is negligible. On the other hand the ohmic admittance DG is very high. As a result of these conditions the voltage on the resonance circuit V_{ne} is more or less constant (see also fig. 4). Fig. 5 shows the absolute value and fig. 6 the locus diagram of the current I_F over the fault location as a function of the Petersen coil position I_{pos} = $B_L E_1$ for a typical 20 kV network ($B_C E_1$ = 150 A, $Y_W E_1$ = 5 A and $1/Y_U$ = 1 Ω).

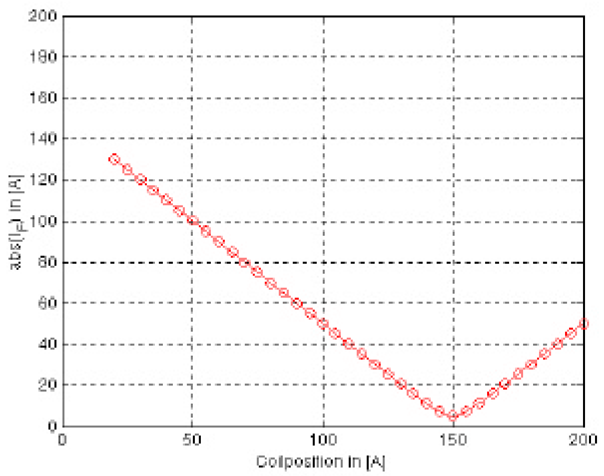

Fig. 5. Absolute value of the current over the fault location I_F.

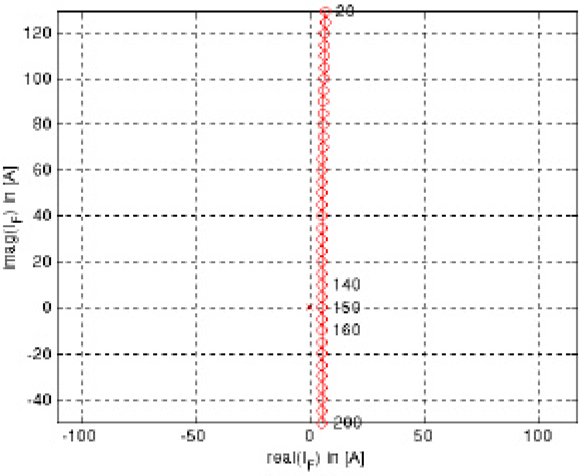

Fig. 6. Locus diagram of the current over the fault location I_F.

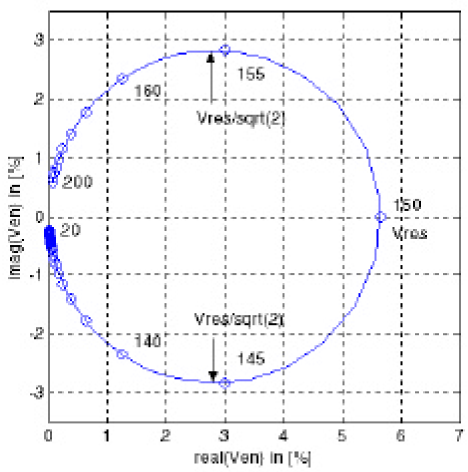

Fig. 8. Locus diagram of the neutral-to-earth voltage V_{ne}.

C. Natural capacitive unbalance of the sound network

In this case the ohmic admittance *DG* is normally negligible compared to the capacitive unbalance jB_C of the network. As a consequence the current I_F is more or less constant (see fig. 4). In analogy to the previous subsection fig. 7 shows the absolute value and fig. 8 the locus diagram of the neutral-to-earth voltage V_{ne} at the fault (unbalance) location as a function of the Petersen coil position $I_{pos} = B_L E_1$ for a typical 20 kV network ($B_C E_1$ = 150 A, $Y_W E_1$ = 5 A and $1/Y_U$ = 40 kΩ).

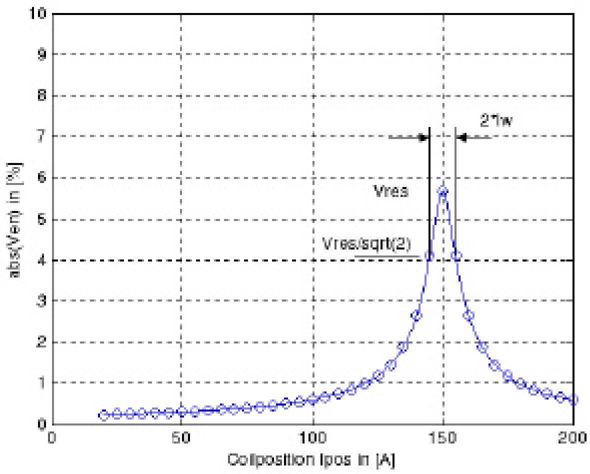

Fig. 7. Absolute value of the neutral-to-earth voltage V_{ne}.

The resonance curve of the sound network can be described by the following three parameters:

V_{res}	maximum voltage of the resonance curve
I_{res}	corresponding coil position to V_{res}
I_w	wattmetric current over the fault location in the case of a low ohmic earth-fault

These parameters can be determined from the resonance curve in an easy way. At the resonance point ($B_C = B_L$) eq. (14) simplifies to

$$V_{res} = -\frac{Y_U}{Y_U + Y_W} E_1 . \tag{15}$$

In order to explain the meaning of the current I_w, let us consider the point of the resonance curve from fig. 7 or fig. 8 where the relation $\left|\frac{V_{ne}}{V_{res}}\right| = \frac{1}{\sqrt{2}}$ holds. Thus, under the assumption $Y_U << Y_W$ the corresponding coil position $I_{pos,W} = B_{L,W} E_1$ can be calculated from eq. (14) in the form

$$\left|\frac{V_{ne}}{V_{res}}\right| = \frac{1}{\sqrt{2}} = \left|\frac{1}{1 + \frac{j(B_C - B_{L,W})}{Y_U + Y_W}}\right| \approx \left|\frac{1}{1 + \frac{j(B_C - B_{L,W})}{Y_W}}\right| \tag{16}$$

or equivalently

$$(B_C - B_{L,W}) = Y_W . \tag{17}$$

Multiplying eq. (17) with E_1, we get the relations

$$(B_C - B_{L,W})E_1 = I_{res} - I_{pos,W} = Y_W E_1 = I_W . \tag{18}$$

Thus, eq. (18) says that the difference between the coil position at the resonance point I_{res} and the coil position $I_{pos,W}$ where the voltage V_{ne} is reduced to $V_{res}/\sqrt{2}$ is equal to the wattmetric current I_W.

For the explanation of the new control algorithm it will be useful to consider the absolute value and the locus diagram of the inverse of the neutral-to-earth voltage

$$\frac{1}{V_{ne}} = -\frac{Y_U + Y_W + j(B_C - B_L)}{Y_U E_1} \tag{19}$$

as presented in the figs. 9 and 10.

III. Disturbances of the Control Operation

Following the previous discussion it seems to be very easy to find the resonance point of the sound network even for very small neutral-to-earth voltages. The problem becomes more difficult because several disturbances generate a non-zero

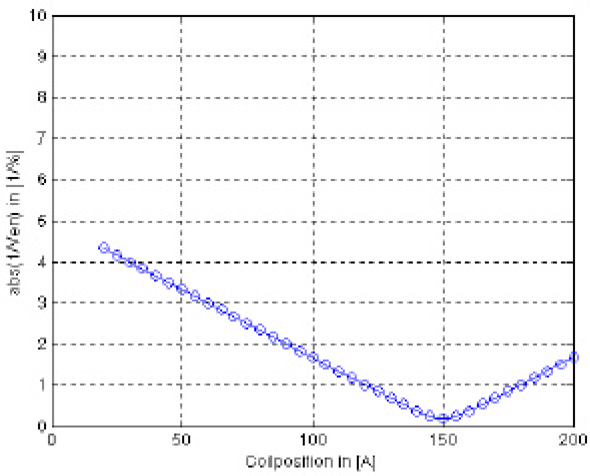

Fig. 9. Absolute value of the neutral-to-earth voltage $1/V_{ne}$.

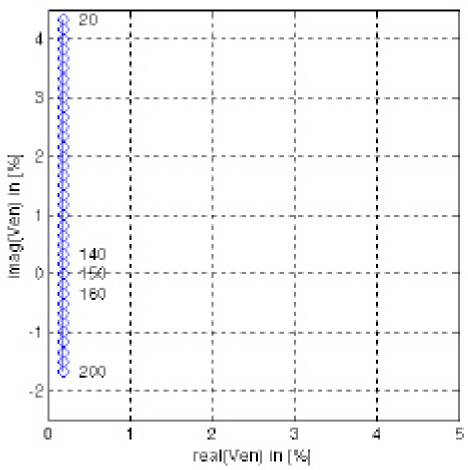

Fig. 10. Locus diagram of the neutral-to-earth voltage $1/V_{ne}$.

neutral-to-earth voltage V_{ne}. Thus, it is very difficult for the control algorithm to distinguish between "real" resonance points and "fictitious" resonance points caused by the disturbances. Next we will discuss the different reasons for the disturbances of the measurement of V_{ne} :

1. High noise levels in the measurement of V_{ne} due to, e.g. inductive and capacitive coupling on the line from the measurement winding of the Petersen coil to the controller. This effect can be reduced, by using twisted and shielded measurement lines.
2. Resolution of the A/D converter. The resonance maximum in cable networks is often less than 0.5 % of E_1. Thus, in order to identify a resonance curve the resolution should be in the range of 0.01 % of E_1.
3. Harmonics in the zero-sequence system. They can be filtered in the controller.
4. Unbalance of the voltage (dE_1) coupled from the HV.
5. Unbalance of the voltage (dE_1) due to manufacturing tolerances of the transformer in the range less than 1 %. As a result a completely balanced HV-system generates an unbalanced system on the MV side.
6. An asymmetric load of the auxiliary system on the tertiary winding of the earthing-transformer (zig-zag) also generates an unbalance of the voltage (dE_1).
7. Capacitive unbalance of the lines due to, e.g. the geometrical arrangement of the phases in overhead lines or due to the manufacturing tolerances of cables.
8. Coupling of the load current over the normally negligible line resistances and reactances (symmetric and asymmetric values).
9. Coupling of the load current over the normally negligible mutual coupled line reactances (symmetric and asymmetric values).
10. Measurement of the neutral-to-earth voltage V_{ne} using the open delta winding at the busbar instead of the auxiliary winding of the Petersen coil results in a constant amplitude and phase error. This is caused by the different accuracy classes of the open delta winding and the transformer.
11. Non-linearity between the measured coil position and the real susceptance of the Petersen coil. The sensor for the coil position is a linear potentiometer, which gives a signal proportional to the air gap. But the susceptance of the Petersen coil is a non-linear function of the air gap.
12. Capacitive coupling from parallel lines of different voltage levels on the same lattice tower. To reduce the required ground floor, lines with different voltage levels are installed on the same lattice tower. Due to this, changes in the balance of one system are capacitively coupled to the second system.
13. Combination of the disturbances mentioned above where unbalanced loads are important.

In order to get an impression of the quantitative influence of some of these disturbances on the neutral-to-earth voltage V_{ne}, in particular 4 to 9, we will subsequently investigate a simple 20 kV network.

A. Description of the network

The network under consideration consisting of a transformer, the Petersen coil, a transmission line and a load is depicted in fig. 11.

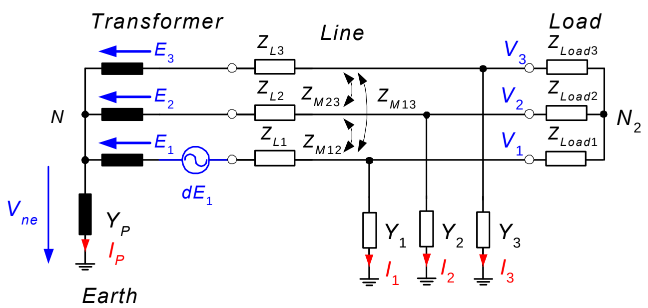

Fig. 11. Simple equivalent circuit for the investigation of some disturbances on the neutral-to-earth voltage V_{ne}.

Let us assume that

- the transformer (110 kV / 20 kV) is ideal with no losses and no leakage inductance,
- the line is 44.5 km long with $z_{M12,\, M23,\, M13} = j\, 0.01665$ Ω/km, $y_{1,2,3} = j9.4251\times10^{-5}$ 1/(Ω km) and $z_{L1,L2,L3}$ = (0.233 + j0.1665) Ω/km,

- the admittance of the Petersen coil has the value Y_P = (0.432 + j 12.987) 1/Ω and
- the load is within the range $Z_{Load1,\ Load2,\ Load3}$ = 38.5 - ∞ Ω.

For the sake of clarity, we further assume without restriction of generality that unbalances of the transmission line only occur in phase 1. Furthermore, the mutual coupling of the transmission lines is neglected because if the network is symmetrical it only has minor influence on the results. The case of asymmetrical mutual coupling can be treated in a similar way as an unbalance in the series reactance of one phase. It is worth mentioning that the equations for a complete description of the different coupling effects of networks with asymmetrical components are very complex and cannot be simplified by using the classical symmetrical component concept (see, e.g. [3] [6] [11]).
The disturbances described in the items 4 to 9 can be reduced to the following three coupling effects, which will be discussed in more detail on the basis of the network of fig. 11:

- Unbalance of the voltage (dE_1).
- Unbalance of the line-to-earth capacitances.
- Coupling of the load current over the normally negligible line resistances and reactances.

B. Coupling phenomena for V_{ne}

1) Unbalance of the voltage dE_1

Under the assumption that all components of the network are symmetrical except for the unbalanced voltage dE_1 we get the following relation between V_{ne} and dE_1

$$\frac{V_{ne}}{dE_1} = -\frac{Y_L Y_C}{3Y_L Y_C + Y_P(Y_L + Y_C)} \qquad (20)$$

with

$Y_L = \dfrac{1}{(R_L + jwL_L)}$	series line admittance
$Y_C = jwC$	line-to-earth capacitive admittance
$Y_P = G_P + \dfrac{1}{jwL_P}$	admittance of the Petersen coil.

The important information of eq. (20) is that even in a network with ideal symmetrical components (line resistances, line reactances, mutual coupling, line-to-earth capacitances and loads) an unbalance dE_1 will produce a non-zero neutral-to-earth voltage V_{ne}. In addition, the amplitude of this voltage depends on different network parameters and has its maximum in the case when the Petersen coil is adjusted. The relation $|V_{ne}/dE_1|$ as a function of the coil position for the network of fig. 11 is shown in fig. 12.

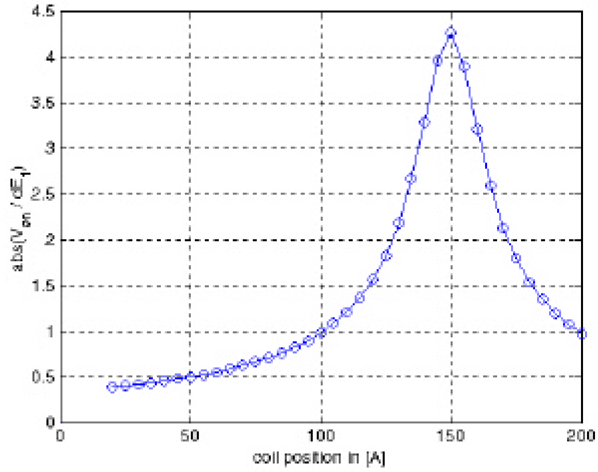

Fig. 12. Neutral-to-earth voltage due to an unbalance on the HV side.

2) Unbalance of the line-to-earth capacitances

For this investigation we assume that dE_1 = 0 and that there is only an unbalance ΔY_C in the line-to-earth capacitance in phase 1. Then the following relation

$$\frac{V_{ne}}{E_1} = -\frac{3{Y_L}^2 \Delta Y_C}{3Y_{n1} + Y_{n2}}$$

$$\frac{V_{ne}}{E_1} = -\frac{3{Y_L}^2 \Delta Y_C}{3Y_{n1} + Y_{n2}} \qquad (21)$$

can be found with

$$Y_{n1} = (Y_C + Y_L + Y_{Load} + \Delta Y_C)(3Y_L Y_C + Y_P(Y_L + Y_C)) \qquad (22)$$
$$Y_{n2} = \Delta Y_C (3{Y_L}^2 + Y_{Load}(Y_P + 3Y_L))$$
$$Y_{Load} = \frac{1}{Z_{Load}}$$
$$\Delta Y_C = jw\Delta C.$$

The natural unbalance in the line-to-earth capacitance ΔY_C also brings about a non-zero neutral-to-earth voltage V_{ne}. But now V_{ne} also depends on the load Y_{Load} and hence on the load current due to the serial impedance of the line. As it can be seen from eq. (21) and eq. (22) this dependence is even present if both the serial line impedance and the load are symmetrical. If there are additional asymmetries in the serial impedances, e.g. due to asymmetrical mutual coupling of the overhead lines, the coupling effect can be worse. Fig. 13 depicts the relation $|V_{ne}/E_1|$ as a function of the load current in the case of an adjusted Petersen coil for the network of fig. 11.

3) Unbalance of the serial impedances of the line

For this calculation the assumption dE_1 = 0 and a symmetrical network except for an asymmetry of 5% in Z_L of phase 1 is made. The mathematical relations for this case are systematically derived by means of a special package written in the computer algebra program MAPLEV (see [7]). Since the formulas are rather complex we restrict ourselves to present the graph of the relation $|V_{ne} / E_1|$ in fig. 14 as a function of the load current in the case of an adjusted Petersen coil for the network of fig. 11.

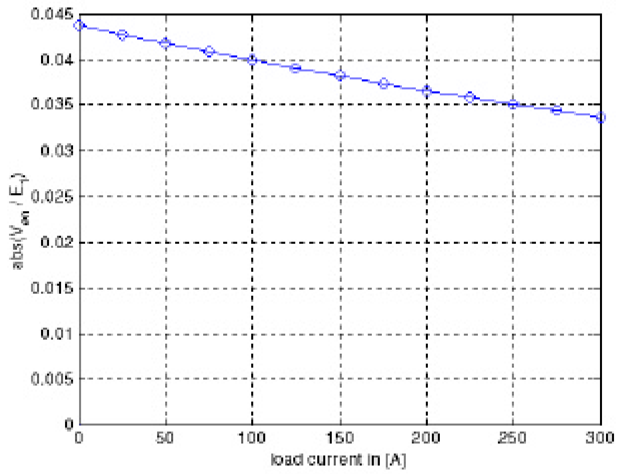

Fig. 13. Neutral-to-earth voltage due to a capacitive unbalance and non-zero serial impedances in the line.

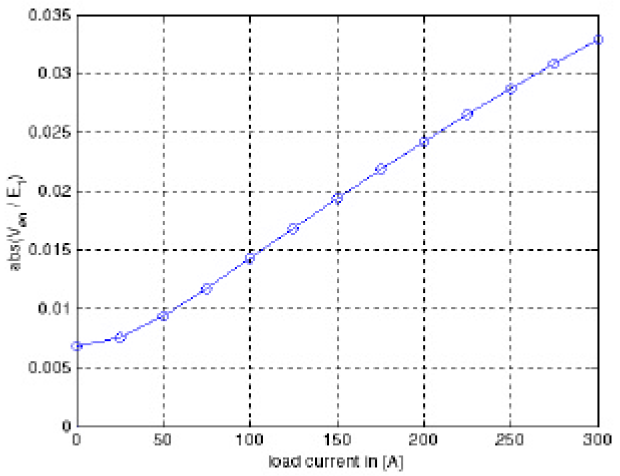

Fig. 14. Neutral-to-earth voltage due to an unbalance of the serial impedances in the line.

The important result is that there is an increasing neutral-to-earth voltage V_{ne} depending on the load current. If the load current is zero V_{ne} results from the capacitive current of the line itself. In some networks the neutral-to-earth voltage is zero in the case of no-load operation of the network. The coupled voltages of the capacitive unbalance and of the unbalance of the serial impedances are compensating themselves. But as it can be seen in fig. 14 the neutral-to-earth voltage V_{ne} is increasing depending on the load.
The asymmetry of a line may be caused for example by the kind of laying the cables, as shown in figure 15a (for further details the reader is referred to [4][10][11]). If the cables are laid in a triangle (see Fig. 15b) the mutual coupling of the three phases is obviously the same. A similar situation can be found for overhead lines where an improvement can be made, by transposing the phases.

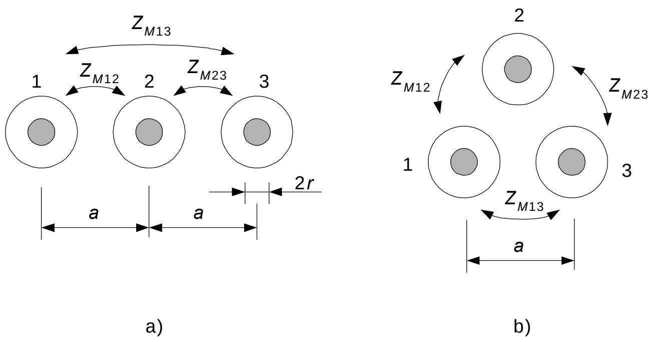

Fig. 15. a) Single conductor cables in parallel.
b) Single conductor cables in triangle.

IV. CONTROL OF THE PETERSEN COIL

The only quantities being measurable for the controller are the actual coil position and the neutral-to-earth voltage V_{ne}. Fig. 16 depicts the controller interface of the Petersen coil.

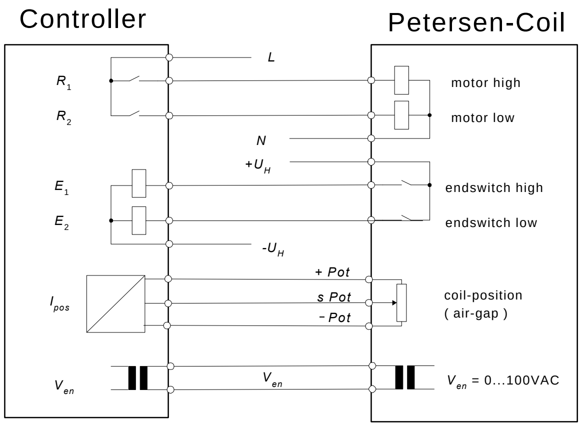

Fig. 16. Controller interface of the Petersen coil.

The task of the controller is to detect a change of the network configuration and to adjust the Petersen coil to the new resonance point or to a predefined over- or under-compensated value [12]. In the simplest version the change of the absolute value of the neutral-to-earth voltage V_{ne} is used as an indication of a switch operation in the network. With this approach not all changes of the network configuration can be detected. An improvement can be made, by investigating the change of the neutral-to-earth voltage V_{ne} in the complex plane [2]. To calculate the resonance curve parameters it is necessary to change the value of the Petersen coil and to measure the corresponding variation of the neutral-to-earth voltage V_{ne}. As shown in the sections before, the voltage V_{ne} is corrupted by different disturbances. Summarizing the objectives, the controller has

- to distinguish between a “real” resonance point and a “fictitious” resonance point, in particular in the case of small neutral-to-earth voltages and
- to recognize switch operations during the tuning operation of the Petersen coil.

It has turned out that by means of a least-squares approach (see, e.g. [8]) the parameters V_{res}, I_{res} and I_W of the resonance curve of fig. 7 can be obtained in a robust way. The Petersen coil needs in its fastest operation mode about 60 s from one end-switch to the other. This requires that during the tuning operation about every 0.5 s a new estimation is accessible. To avoid too high computational consumption the non-linear parameter estimation problem is transformed to a linear one. For this purpose let us consider eq. (19) in the form

$$\left|\frac{V_{ne}}{E_1}\right|^2 = \frac{1}{|T|^2} = \frac{1}{\left(1+\frac{Y_W}{Y_U}\right)^2 + \left(\frac{B_C - B_L}{Y_U}\right)^2} \quad (23)$$

or equivalently

$$0 = Y_U^2 + 2Y_U Y_W + Y_W^2 + B_C^2 - 2B_C B_L - Y_U^2 |T|^2 + B_L^2. \quad (24)$$

Since $|T|^2$ and B_L can be measured, we can rewrite eq. (24) for n different measurement points in the form

$$\begin{bmatrix} -2B_L & -|T|^2 & 1 \\ \cdots & \cdots & \cdots \\ \cdots & \cdots & \cdots \\ -2B_L & -|T|^2 & 1 \end{bmatrix}_{1 \ldots n} \begin{bmatrix} x_1 \\ x_2 \\ x_3 \end{bmatrix} = \begin{bmatrix} -B_L^2 \\ \cdots \\ \cdots \\ -B_L^2 \end{bmatrix} \quad (25)$$

with the abbreviations

$$x_1 = B_C \quad (26)$$

$$x_2 = Y_U^2 \quad (27)$$

$$x_3 = Y_U^2 + 2Y_U Y_W + Y_W^2 + B_C^2. \quad (28)$$

Eq. (25) can be solved with a classical least squares approach in order to obtain B_C, Y_U and Y_W and from this the parameters V_{res}, I_{res} and I_W for the construction of the resonance curve. It is worth mentioning that for the sake of computational efficiency an on-line version of the least-squares algorithm is implemented [8]. However, some further steps in the preprocessing of the signals have to be taken to gain additional robustness against disturbances.

V. Results Of Field Tests

In the meantime the new algorithm is implemented in a real hardware and has shown his advantages in real network configurations. As an example fig. 17 shows the estimated inverse resonance curve (see eq. (19) and fig. 9), by using only the marked samples from the measured values for the computation of the parameters. The real resonance point of the network is at 100 A. The accuracy obtained is sufficient for the required tuning.

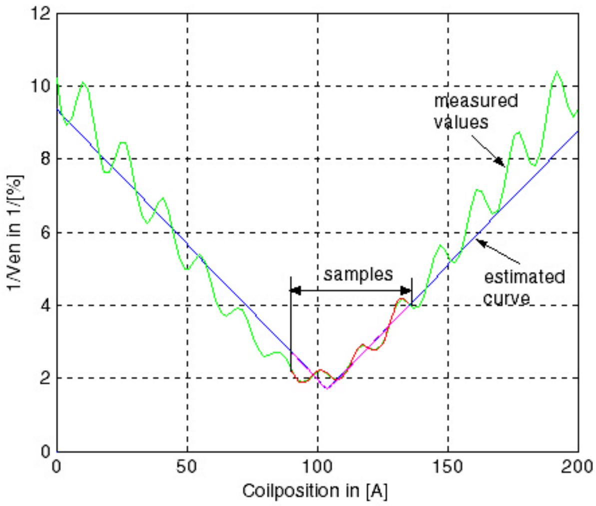

Fig. 18. Inverse resonance curve estimated from the sampled values.

VI. Conclusion

In this contribution we have discussed the principle of “resonant grounding” and the effect of different disturbances on the measurements. A prerequisite for an automatic control operation of the Petersen coil is an unbalance in the network in order to get a non-zero neutral-to-earth voltage. To see the limits of this concept, we have elaborated the different disturbances, which may occur in every real-world network. According to these requirements we have presented a new algorithm to reduce the influence of the disturbances. The field test and the first practical experiences show the effectiveness of this new concept for the control of Petersen coils.

References

[1] DIN VDE 0228, *Maßnahmen zur Beeinflussung von Fernmeldeanlagen durch Starkstromanlagen*, 1987.

[2] Druml G., *Resonanzregler REG-DP, Betriebsanleitung*, a-eberle gmbh Nürnberg, 2001.

[3] Grainger J., Stevenson W., Jr., *Power System Analysis*, McGraw-Hill, Singapore, 1994.

[4] Heinhold L., *Kabel und Leitungen für Starkstrom*, Siemens, Berlin-München, 4.Aufl., 1987.

[5] Hubensteiner H., *Schutztechnik in elektrischen Netzen 1*, VDE Verlag, Berlin-Offenbach, 1993.

[6] Koettnitz H., Pundt H., *Berechnung elektrischer Energieversorgungs- netze, Mathematische Grundlagen und Netzparameter*, VEB Deutscher Verlag für Grundstoffindustrie, Leipzig, 1973.

[7] Kugi A., Schlacher K., Kaltenbacher M., *Object oriented approach for large circuits with substructures in the computer algebra program Maple V*, In: Software for Electrical Engineering Analysis and Design, Ed.: Silvester P.P., pp. 490-500, Computational Mechanics Publica-tions, Southampton, 1996.

[8] Ljung L., System Identification: Theory for the User, Prentice Hall, New Jersey, 1987.

[9] Poll J., *Löschung von Erdschlusslichtbögen,* In: Elektrizitätswirtschaft, Jg.83 (1984), Heft 7, pp 322-327, VWEW-Verlag, Frankfurt am Main

[10] VDEW: *Kabelhandbuch,* VWEW-Verlag, Frankfurt am Main, 1997.

[11] Weßnigk K., *Kraftwerkselektrotechnik*, VDE Verlag, Berlin-Offenbach, 1993.

[12] Willheim R., Waters M., *Neutral Grounding in High-Voltage Trans-mission*, Elsevier Publishing Company, London, 1956.